Topographic Organization of Inferior Olive Cells Projecting to Translational Zones in the Vestibulocerebellum of Pigeons

NATHAN A. CROWDER, IAN R. WINSHIP, AND DOUGLAS R.W. WYLIE*
Department of Psychology, University of Alberta, Edmonton, Alberta T6G 2E1, Canada

ABSTRACT

In the nodulus and ventral uvula of pigeons, there are four parasagittal zones containing Purkinje cells responsive to patterns of optic flow that results from self-translation along a particular axis in three-dimensional space. By using a three-axis system to describe the preferred direction of translational optic flow, where $+X$, $+Y$, and $+Z$ represent rightward, upward, and forward self-motion, respectively, the four cell types are: $+Y$, $-Y$, $-X-Z$, and $-X+Z$ (assuming recording from the left side of the head). The $-X-Z$ zone is the most medial, followed in sequence by the $-X+Z$, $-Y$ zone, and the $+Y$ zones. In this study, we injected the retrograde tracer cholera toxin subunit B into each of the four translational zones to determine the origin of the climbing fiber inputs in the inferior olive. Retrograde labeling in the inferior olive was found in the ventrolateral margin of the medial column from injections into all four translational zones; however, there was a clear functional topography. Retrograde labeling from $-Y$ zone injections was found most rostrally in the medial column, whereas retrogradely labeled cells from $-X-Z$ zone injections were found most caudally in the medial column. Labeling from $+Y$ and $-X+Z$ zone injections were found between the labeling from $-Y$ zones and $-X-Z$ zones, with $+Y$ labeling located slightly caudal to $-X+Z$ labeling. J. Comp. Neurol. 419:87–95, 2000.   © 2000 Wiley-Liss, Inc.

Indexing terms: climbing fiber; optokinetic; nodulus; inferior olive; cholera toxin B

As organisms move through an environment containing numerous stationary visual stimuli, "flowfields" or "optic flow" occurs across the entire retina (Gibson, 1954). Motion of any object through three-dimensional space, including self-motion of organisms, can be described with reference to six degrees of freedom: three of translation, and three of rotation. Self-rotation and self-translation result in distinctive patterns of optic flow (see Fig. 1C,D). Previous electrophysiological studies in pigeons have shown that the vestibulocerebellum (VbC) can be divided into two parasagittal zones based on responses to optic flow stimuli (Wylie et al., 1993). Medially in the VbC (nodulus and ventral uvula), complex spike (CS) activity of Purkinje cells responds best to optic flow resulting from self-translation, whereas cells in the lateral VbC (flocculus) respond best to optic flow resulting from self-rotation. There are two types of rotation cells: cells that prefer rotation about the vertical axis (VA neurons), and cells that prefer rotation about a horizontal axis oriented at 135 degrees ipsilateral azimuth (H-135 neurons; Wylie and Frost, 1993). Translational cells can be classified into four

types based on the preferred axis of translational optic flow: $+Y$, $-Y$, $-X-Z$, and $-X+Z$ cells (where $+X$, $+Y$, and $+Z$ represent upward, rightward, and forward self-motion, respectively, and assuming recording from the left side of the head; Wylie et al., 1998; Wylie and Frost, 1999). The preferred axis of translation for $+Y$, $-Y$, $-X-Z$, and $-X+Z$ neurons is shown in Figure 1. $+Y$ cells respond best to optic flow that results from movement of the bird upwards; i.e., a flowfield consisting largely of downward motion, and a focus of expansion (FOE) above the bird's head along the vertical (Y) axis. Conversely, $-Y$ cells respond best to optic flow that results from movement of the bird

ABBREVIATIONS

CS	complex spike
CF	climbing fiber
CTB	cholera toxin subunit-B
DAB	diaminobenzidine
dl	dorsal lamella
FOE	focus of expansion
IO	inferior olive
LM	lentiformis mesencephali
LTN	lateral terminal nuclei
mc	medial column
MTN	medial terminal nuclei
nBOR	nucleus of the basal optic root
NOT	nucleus of the optic tract
nXII	nucleus of the twelfth nerve
VbC	vestibulocerebellum
vl	ventral lamella
XII	twelfth nerve

Fig. 2. Location of translation cells in the pigeon vestibulocerebellum (VbC). This view of the VbC seen in the coronal plane illustrates the organization of translation cells in the nodulus (folium X) and ventral uvula (ventral lamella of folium IXc,d). The four sagittal zones, from medial to lateral, illustrate the locations of $-X-Z$, $-X+Z$, $-Y$, and $+Y$ Purkinje cells, respectively (Wylie and Frost, 1999). Scale bar = 1 mm.

downwards. $-X-Z$ cells respond best to the optic flow that results from self-motion (backwards) along an horizontal axis that is oriented at 135° ipsilateral azimuth. $-X+Z$ cells respond best to the optic flow that results from self-motion (forwards) along an horizontal axis that is oriented at 45° ipsilateral azimuth. Self-motion along this axis produces optic flow with a FOE at 45 ° ipsilateral azimuth.

The translational cells are segregated medial-laterally into parasagittal zones. Moving medial to lateral, the zones are $-X-Z$, $-X+Z$, $-Y$, $+Y$, respectively (see Fig. 2). In pigeons, the climbing fiber (CF) input to the VbC is from the medial column (mc) of the inferior olive (IO; Arends and Voogd, 1989). Lau et al. (1998), by using pressure injections of the retrograde tracer cholera toxin subunit B (CTB), found that the inputs to translational and rotational zones of the VbC are located in ventrolateral and dorsomedial mc, respectively. More recently, by making small injections of CTB with iontophoresis, Wylie et al. (1999) showed that cells providing CF input to H-135 and VA cells in VbC were located in the rostral and caudal parts of the dorsomedial mc, respectively. In this study, we investigated inferior olive projections to each of the four translational zones in the VbC by using iontophoretic injections of CTB.

MATERIALS AND METHODS
Surgery

The methods reported herein conform to the guidelines established by the Canadian Council on Animal Care and were approved by the Biological Sciences Animal Services at the University of Alberta. Silver King and Racing
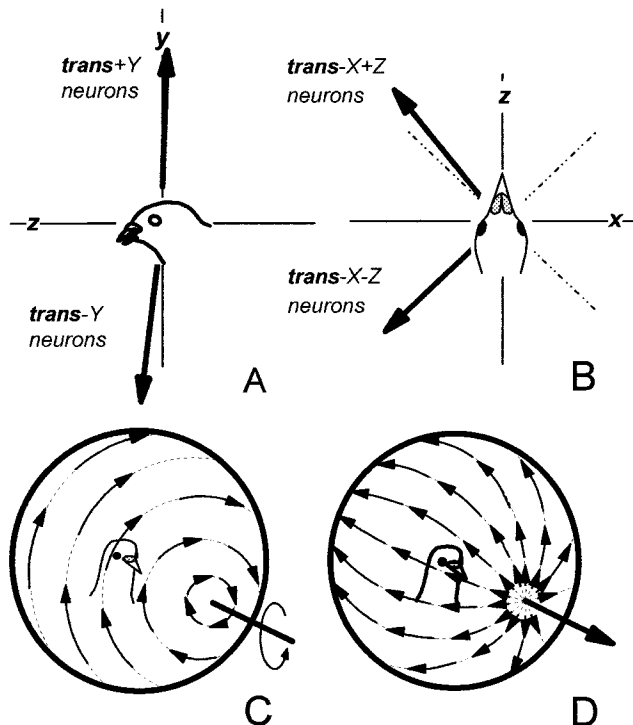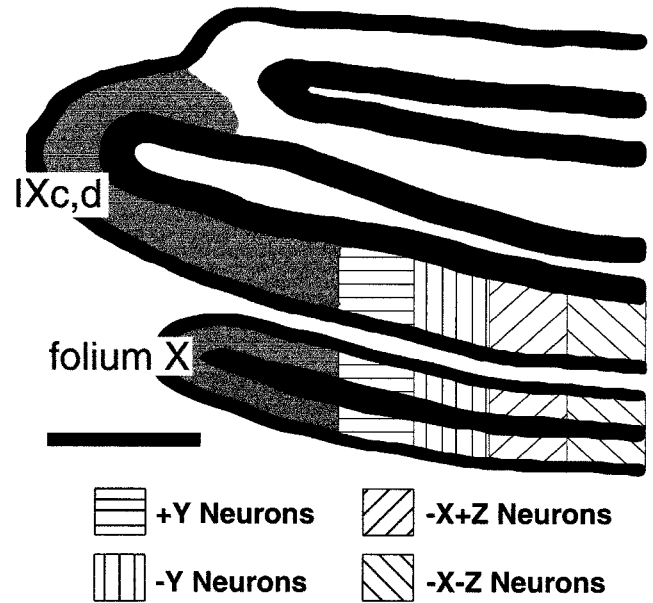

Fig. 1. The four types of translation cells in the vestibulocerebellum. The arrows in both **A** and **B** indicate the preferred axes of translation-sensitive neurons in the nodulus and ventral uvula (from Wylie et al., 1998; Wylie and Frost, 1999). The arrows represent the direction of self-motion of the bird that would result in the flowfield causing maximal excitation. That is, the arrows point to the focus of expansion (FOE) in the flowfield. The four types of translation-sensitive neurons are: $-X-Z$, $-X+Z$, $+Y$, and $-Y$ (assuming, recording from the left side of the head; where $+X$, $+Y$, and $+Z$ represent movement of the bird's head right, up, and forward, respectively). A shows the preferred axis of $+Y$ and $-Y$ neurons as seen in the sagittal plane, B shows the preferred axis of $-X-Z$ and $-X+Z$ neurons as seen in the horizontal plane. **C** and **D** show rotational and translational optic flowfields, respectively, resulting from rotation about, or translation along, the z axis. The arrows on the sphere surrounding the pigeon represent local image motion in the flowfield.

Homer pigeons were anesthetized with a ketamine (75 mg/kg)/xylazine (10 mg/kg) cocktail injected intramuscularly; supplemental doses were administered as necessary. Animals were placed in a stereotaxic device with pigeon ear bars and beak adapter such that the orientation of the skull conformed to the atlas of Karten and Hodos (1967). The dorsal surface of the auricle of the cerebellum was exposed by removing sections of bone and dura in the area contained by the anterior canal of the vestibular apparatus.

Extracellular recordings were made with glass micropipettes (4 μm tip diameter, containing 2 M NaCl) that were oriented 35°–45° to the sagittal plane. After CS activity of Purkinje cells in the nodulus or ventral uvula was isolated, the optic flow preference was determined by moving a large (90°×90°) hand-held stimulus in various areas of the visual field and by monitoring responses to flowfield stimuli produced by the planetarium and translator projectors described previously (Wylie and Frost, 1993; Wylie et al., 1998). After identification of a translational flowfield preference, the recording electrode was replaced with a micropipette (10–16 μm tip diameter) containing low-salt CTB (1% in 0.1 M phosphate-buffered saline (PBS) pH 7.4; Sigma, St. Louis, MO). CS activity was once again recorded to confirm the cell type before the solution was iontophoretically injected (+3 μA, 7 seconds on, 7 seconds off) for 3–10 minutes. Following CTB injection, the electrode was left undisturbed for an additional 5 minutes.

Processing for cholera toxin subunit B

After a survival time of 3–5 days, the animals were given an overdose of sodium pentobarbitol (100 mg/kg) and immediately perfused with saline (0.9%) followed by ice-cold paraformaldehyde (4% in 0.1 M phosphate buffer [PB] pH 7.4). Brains were extracted and postfixed for 2–12 hours (4% paraformaldehyde, 20% sucrose in 0.1 M PB), and cryoprotected in sucrose overnight (20% in 0.1 M PB). Frozen sections, 45-μm-thick, were collected in the coronal plane, then washed in PBS. In some cases, if the perfusion was less than ideal, sections were washed for 30 minutes in a 25% methanol/30% hydrogen peroxide solution to decrease endogenous peroxidase activity.

The CTB protocol used was based on Wild (1993). Tissue was incubated for 30 minutes in 4% rabbit serum (Sigma) with 0.4% Triton X-100 in PBS, followed by goat anti-CHB (List Biological Laboratories, Campbell, CA; 1:20,000) for 20–24 hours at 4°C. The sections were then washed with 0.1 M PBS and placed in biotinylated rabbit anti-goat antiserum (Vector Laboratories, Burlingame, CA; 1:600) with 0.4% Triton X-100 in PBS for 1 hour. Sections were washed in PBS, then incubated for 90 minutes in Extravidin peroxidase (Sigma; 1:1,000) with 0.4% Triton X-100, then rinsed again in PBS. Tissue was visualized using diaminobenzidine (DAB). After a 10-minute incubation in 0.025% DAB and 0.006% $CoCl_2$ in 0.1 M PBS, 0.005% hydrogen peroxide was added, and the tissue was reacted for up to 2 minutes. The tissue was subsequently washed 4–6 times in PBS, mounted onto gelatin chrome aluminum-coated slides, lightly counterstained with Neutral Red, coverslipped with Permount, and examined by using light microscopy.

Nomenclature

The IO of pigeons consists of a dorsal (dl) and ventral (vl) lamella, which are joined by the mc (Vogt-Nilson,
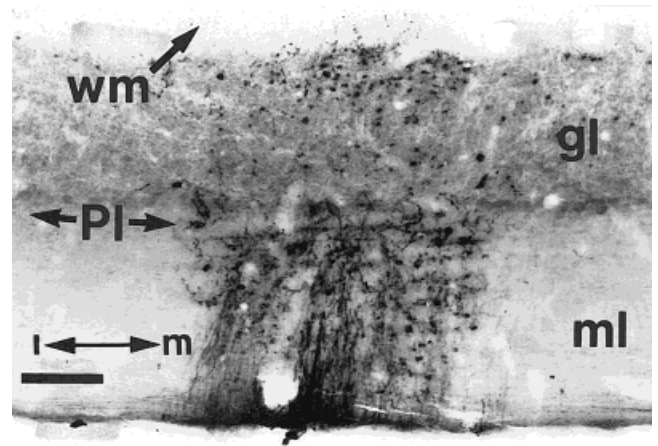

Fig. 3. The injection site in the ventral lamella of folium IXc,d from case 4. The granular layer (gl), Purkinje layer (Pl), molecular layer (ml), and white matter (wm) are indicated. Most apparent from the injection sites was labeling of climbing fibers and Purkinje cell dendrites extending into the molecular layer. Some labeling of parallel fibers and granule cells was also observed. Scale bar = 100 μm.

1954). The avian cerebellum consists of a vermis, without the characteristic hemispheres of mammalian species (Larsell, 1948; Larsell and Whitlock, 1952; Whitlock, 1952). The VbC of pigeons includes the two most ventral folia of the posterior vermis. These are referred to as IXc,d and X (Karten and Hodos, 1967), which we adopt, or IXb and X (Arends and Zeigler, 1991). In general, folia IXc,d and X are referred to as the uvula and nodulus, respectively (Larsell, 1948; Larsell and Whitlock, 1952; Whitlock, 1952). These folia extend laterally to form the auricle of the cerebellum, which has been referred to as the paraflocculus or flocculus (Larsell, 1948; Larsell and Whitlock, 1952; Whitlock, 1952). Based on the responses of Purkinje cell CS activity to optic flow stimuli (Wylie et al., 1993), we have divided the VbC into a rotation zone which we refer to as the flocculus, and a translation zone we refer to as the nodulus and ventral uvula (see Fig. 2). Unlike the gross anatomical distinction between flocculus and nodulus in mammals, the distinction in pigeons is based on physiological recordings (Wylie et al., 1993).

RESULTS

Injections were made in 10 pigeons. Three pigeons received bilateral injections, providing 13 cases in total. Figure 3 shows a typical injection site. It is characterized by the labeling of Purkinje cell dendrites and CFs in the molecular layer. Generally the injections sites were about 60–200 μm in width, although with the widest injection there was diffuse labeling up to 250 μm from the center. Some granular cells local to the injection were also labeled. There were three injections to the −X−Z zone (case 2, right side; case 2, left side; case 4). Two of the injections were localized to the ventral lamella of folia X (case 2, right side; case 4) and the other was found in dorsal X (case 2, left side). On average, these injections were located about 200 μm from the midline (188 ± 63 μm; mean ± S.E.M.). There were three cases where the +Y zone was injected (case 1; case 12, right side; case 12, left

side). Two of the injections were localized to the ventral lamella of folia IXc,d (case 1; case 12, left side) and the other was found in ventral X (case 12, right side). On average, these injections were located about 1,900 μm from the midline (1,870 ± 217 μm). The −X+Z zone was injected in four cases (case 3, left side; case 5; case 8, left side; case 10). Three of the injections were localized to the ventral lamella of folia X (case 3, left side; case 5; case 10) and the other was found in dorsal X (case 8, left side). On average, these injections were located about 1,200 μm from the midline (1,160 ± 293 μm). There were three injections to the −Y zone (case 3, right side; case 8, right side; case 13). Two of the injections were localized to the dorsal lamella of folia X (case 8, right side; case 13) and the other was found in ventral X (case 3, right side). On average, these injections were located about 1,300 μm from the midline (1,308 ± 114 μm). The locations of the physiologically distinct cell types match well with previous recording data (Wylie et al., 1993; see Fig. 2).

In all cases, retrogradely labeled cells were found contralateral to the injection site in the ventrolateral regions of the mc. The number of retrogradely labeled cells found ranged between 31 and 169. A distinct rostral-caudal segregation between retrogradely labeled cells from different translational zones was observed. The rostralmost tip of the twelfth nucleus (nXII) was used as a landmark to compare rostral-caudal distributions of cells between different cases.

−X−Z labeling

Compared to the other zones, retrograde labeling from injections into the −X−Z zone was the least diffuse. Dense clusters of labeled cells were found approximately 1 mm caudal to the rostral tip of nXII. These cells were found just medial to, just lateral to, and amongst the stria of the twelfth nerve (XII; see Figs. 4D, 5D). In case 2 (right side), there were 45 retrogradely labeled cells. They were distributed from 480 to 1,270 μm caudal to the rostral tip of nXII, but a cluster containing 80% of the total was found in the caudal end of this distribution (790−1,100 μm caudal to the rostral tip of nXII). In case 2 (left side) there were 97 retrogradely labeled cells, distributed from 480 to 1,230 μm caudal to the landmark section. As with the right side, the majority (93%) were found in the caudal part of the distribution (660−1,200 μm caudal to the landmark section). In case 4, there were 87 retrogradely labeled cells, found in a cluster distributed from 790 to 1,230 μm caudal to the landmark section. In summary, these three injections resulted in clusters of labeled cells centered 900−1,000 μm caudal to the rostral tip of nXII. Figure 4D shows a series of drawings from case 2 (right side) of coronal sections through the mc illustrating the labeling typical of a −X−Z zone injection. Figure 5D shows a photomicrograph of labeled cells in the caudal mc from a −X−Z zone injection.

−Y labeling

The distributions of retrogradely labeled cells from injections into the −Y, +Y, and −X+Z zones were more diffuse than those of the −X−Z zone. Moreover, the distributions resulting from injections into these three zones overlapped to a certain degree (see Fig. 4A–C). Nonetheless, there was a clear rostrocaudal segregation of the distributions. Retrogradely labeled cells from injections into the −Y zone were located most rostrally in the mc.

Dense clusters of labeled cells were located approximately 0.2–0.5 mm rostral to the rostral tip of nXII. The majority of these cells were found lateral to XII (see Figs. 4A, 5A). In case 3 (right side), there were 40 retrogradely labeled cells found, 90 μm caudal to 480 μm rostral to the rostral tip of nXII. This distribution was skewed rostrally, as about half (48%) of the total was found 130−310 μm rostral to the rostral tip of nXII. In case 8 (right side), there were 96 retrogradely labeled cells. They were distributed throughout the rostrocaudal extent of mc (from 1,190 μm caudal to 530 μm rostral to the landmark section); however, a dense cluster containing 51% of the total was found 130−400 μm rostral to the rostral tip of nXII. In case 13, there were 31 retrogradely labeled cells, distributed from 260 to 660 μm rostral to the rostral tip of nXII. A cluster containing 84% of the total was found 350−570 μm rostral to the rostral tip of nXII. Figure 4A shows a series of drawings of coronal sections (case 13) through the mc illustrating the labeling typical of a −Y zone injection. Figure 5A shows a photomicrograph of labeled cells in the mc from a −Y zone injection.

+Y labeling

Of all the distributions, labeled cells resulting from CTB injections in the +Y and −X+Z zones overlapped to the greatest degree. Labeling resulting from injections into the +Y zone was found near the middle of the rostrocaudal extent of mc. The majority of cells were found just medial to, and amongst the stria of XII (see Figs. 4C, 5C). In case 1, there were 154 retrogradely labeled cells, distributed from 660 μm caudal to 130 μm rostral to the rostral tip of nXII. In case 12 (right side), there were 135 labeled cells. They were distributed over a broad range, from 310 μm caudal to 480 μm rostral to the rostral tip of nXII; however, this distribution was skewed caudally: 31% of the total was found 220 μm caudal to 40 μm rostral to the rostral tip of nXII. The distribution of labeled cells from case 12 (left side) was also quite diffuse. There were 169 labeled cells, distributed from 570 μm caudal to 660 μm rostral to the rostral tip of nXII; however, a cluster containing 58% of the total was found ranging from the landmark section to 350 μm caudal to the rostral tip of nXII. In summary, these three injections resulted in retrogradely labeling centered 0.1–0.3 mm caudal to the landmark (case 1: 260 μm caudal; case 12, right side: 100 μm caudal; case 12 (left side): 150 μm caudal). Figure 4C shows a series of drawings (from case 12, right side) of coronal sections through the mc illustrating the labeling typical of a +Y zone injection. Figure 5C shows a photomicrograph of labeled cells in the mc from a +Y zone injection.

−X+Z labeling

Retrogradely labeled cells from injections into the −X+Z zone were found slightly rostral to those cells labeled by the +Y injections. Prominent clusters of labeled cells were located slightly caudal to the rostral tip of nXII. These cells were found just medial to, just lateral to, and amongst the stria of XII (see Figs. 4D, 5D). Labeled cells from −X+Z injections were, on average, about 100 μm lateral to labeled cells from +Y injections. In case 3 (left side), there were 103 labeled cells, distributed from 350 μm caudal to 480 μm rostral to the rostral tip of nXII. In case 5, there were 62 labeled cells. They were distributed from 570 μm caudal to 260 μm rostral to the rostral tip of nXII, although a cluster containing 71% of the total was in
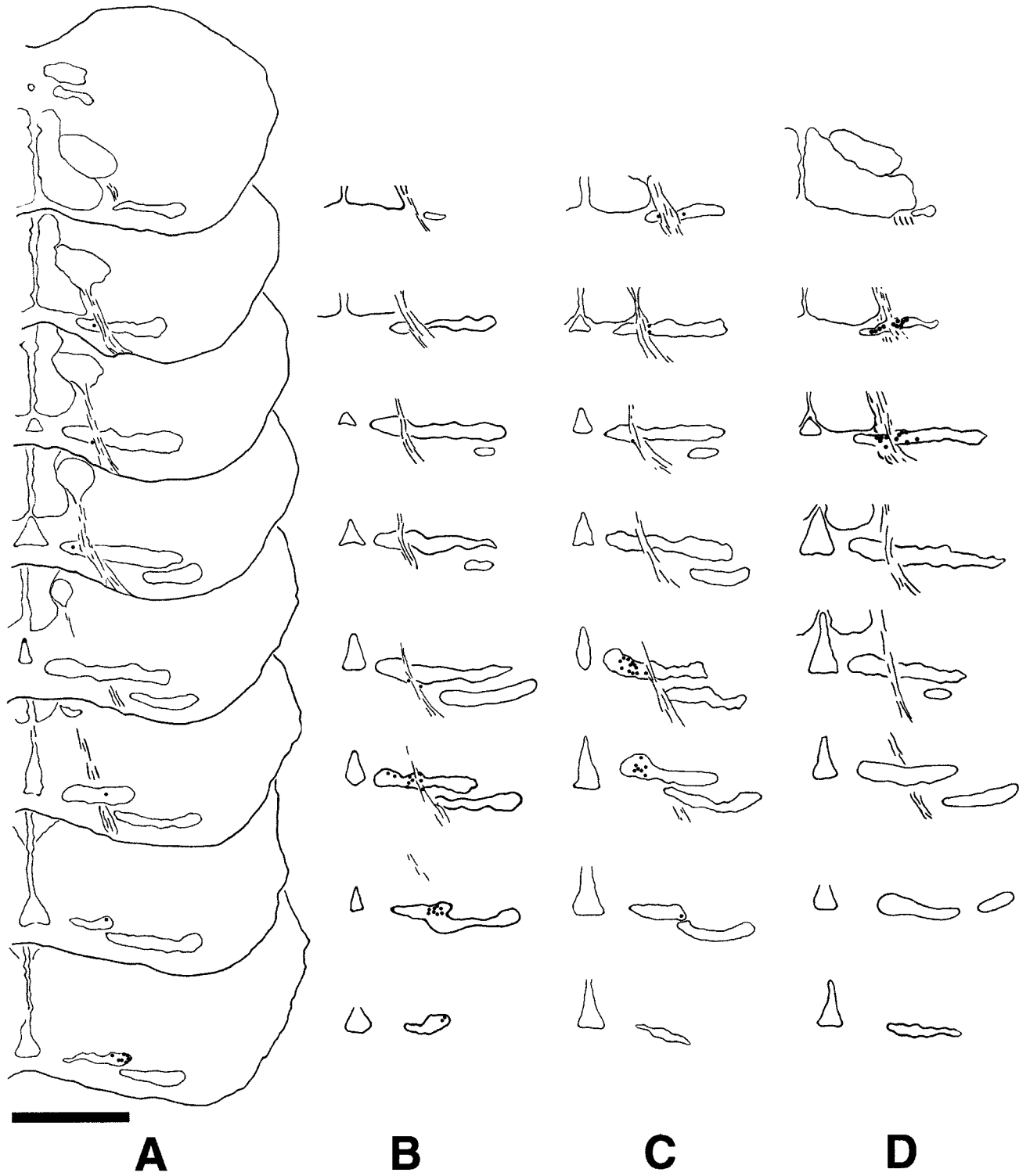
Fig. 4. Labeled cells from cholera toxin subunit-B (CTB) injections into translational zones. A–D show coronal sections (approximately 260 μm apart) through the caudal-rostral extent of the inferior olive (IO) illustrating the location of retrogradely labeled cells resulting from injections of CTB into the: (**A**) −Y (case 13); (**B**) −X+Z (case 3); (**C**) +Y (case 12); and (**D**) −X−Z (case 2) zones of the vestibulocerebellum. A shows the entire section, whereas B–D only show the IO. Scale bar = 1 mm.
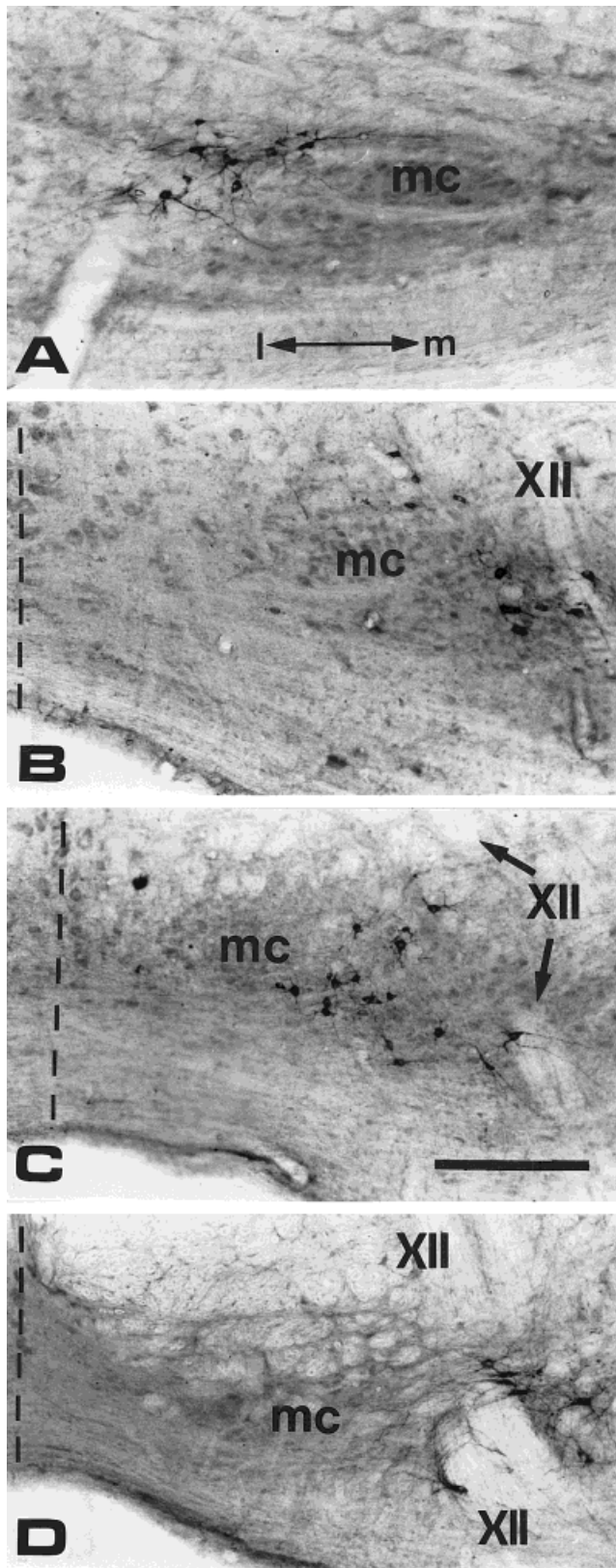
the central 300 µm of this range. In case 8 (left side), there were 71 labeled cells distributed over a broad range from 880 µm caudal to 310 µm rostral to the rostral tip of nXII. This distribution was skewed such that a cluster containing 42% of the total was found 180–400 µm caudal to the rostral tip of nXII. In case 10, there were 53 labeled cells. They were distributed from 440 µm caudal to 220 µm rostral to the rostral tip of nXII, but a cluster containing 43% of the total was found in two coronal sections about 200 µm caudal to the rostral tip of nXII. In summary, the four injections resulted in retrograde labeling centered near the landmark (case 3, left side: 60 µm rostral; case 5: 40 µm caudal; case 8: 100 µm caudal; case 10: 200 µm caudal). Figure 4B shows a series of drawings (from case 3) of coronal sections through the mc illustrating the labeling typical of a −X+Z zone injection. Figure 5B shows a photomicrograph of labeled cells in the mc from a −X+Z zone injection.

DISCUSSION
Topographic organization of the medial column in pigeons

Previous studies had shown that the CF input to the VbC in pigeons is from the mc (Arends and Voogd, 1989). Lau et al. (1998) showed that the rotation zones in the lateral VbC (flocculus) receive CF input from the medial margin of mc, whereas the translation zones in the medial VbC (ventral uvula and nodulus) receive CF input from the lateral margin of the mc. In the present study, we have shown that the region of the lateral mc projecting to the four translation zones of the pigeon VbC is topographically organized. Injections of the retrograde tracer CTB into the most medial zone of the VbC, the −X−Z zone, resulted in retrograde labeling in the extreme caudolateral margin of the mc. Retrograde labeling from injections into the other three zones resulted in overlapping distributions located more rostrally in the lateral mc (some of the overlap we observed could be due to the injections encroaching upon adjacent zones). Of these three zones, retrogradely labeled cells from injections into the −Y zone were clearly located the most rostral in the mc. Labeling from the −X+Z zones was found slightly caudal to the −Y cells, and the distribution of cells from the +Y zone injections was located just caudal and slightly medial to the −X+Z cells.

Recently, Wylie et al. (1999) revealed the functional topography of the CF input from the mc to the rotation zones in the VbC. There are two types of rotation cells in the lateral VbC (Wylie and Frost, 1993). VA cells prefer optic flow resulting from rotation about the vertical (z) axis in the direction producing forward (temporal to nasal;

Fig. 5. Photomicrographs of retrograde labeling in contralateral inferior olive resulting from cholera toxin subunit-B (CTB) injections. A–D show labeled cells resulting from CTB injections into vestibulocerebellar zones −Y (case 8, right side), −X+Z (case 3, left side), +Y (case 1), and −X−Z (case 2, left side), respectively. The sections were located 180 µm rostral (**A**), 0 µm (**B**), 350 µm caudal (**C**), and 700 µm caudal (**D**) relative to the landmark section (rostral tip of the nucleus of the twelfth nerve). Medial column (mc) and twelfth nerve (XII) are indicated. The dotted line represents the midline. The midline for A is located about 50 µm medial to the right edge of the photograph. Scale bar = 200 µm.

Rotation

⊞ VA Cells

⊠ H-135 Cells

Translation
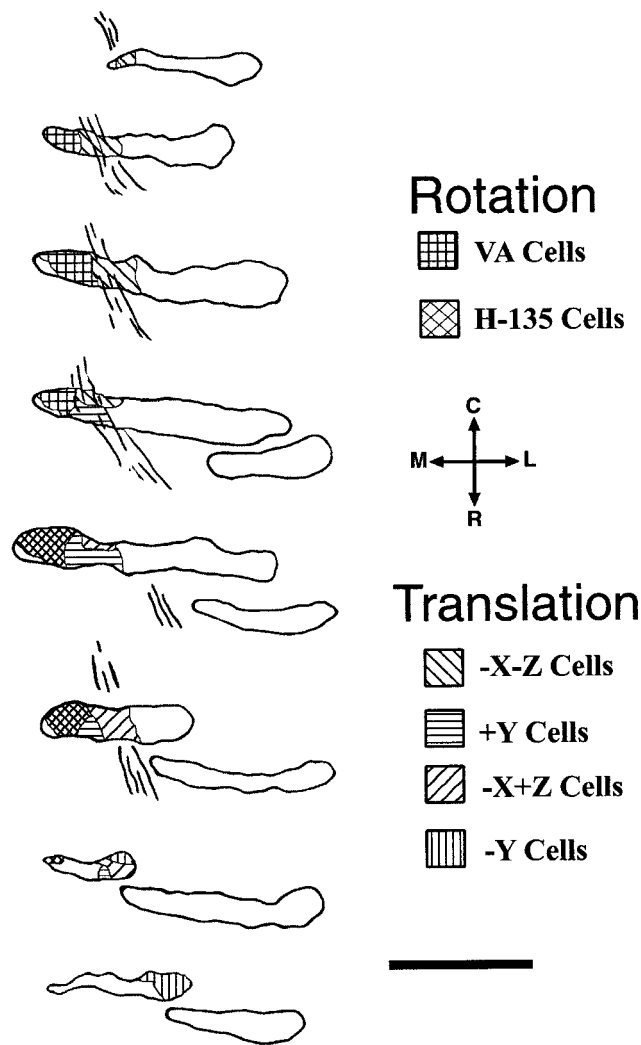
▨ -X-Z Cells

☰ +Y Cells

▨ -X+Z Cells

▥ -Y Cells

Fig. 6. Summary diagram showing the topographical organization of translation and rotation cells in the inferior olive (IO). Different patterns of hatching are used to illustrate the organization of neurons labeled from cholera toxin-B injections into various visually responsive zones in the vestibulocerebellum. This figure is an idealization; although there is overlap between domains (specifically −Y, +Y, and –X+Z), none is shown for the purpose of simplicity. The drawings represent the caudal-rostral extent of the IO. The data for vertical axis (VA) and H-135 cells are from Wylie et al. (1999). Scale bar = 500 μm.

F) motion in the ipsilateral hemifield, and backward motion (nasal to temporal; B) in the contralateral hemifield (see Fig. 7). H-135 neurons prefer optic flow resulting from rotation about an horizontal axis that is oriented at 135° ipsilateral/45° contralateral azimuth and in the direction producing downward motion throughout most of the contralateral hemifield, upward motion in the ipsilateral hemifield, and upward motion in the frontal fields of both eyes. (This organization of neurons preferring rotational optic flow was first noted in rabbits; Simpson et al., 1981; Graf et al., 1988.) Wylie et al. (1999) found that the VA and H-135 received CF input from the caudal and rostral margins of the medial mc, respectively. Figure 6 summarizes the findings of the present study and Wylie et al.

(1999) to illustrate the topographic projection of the pigeon mc to the rotation and translation zones in the VbC. The −X−Z cells are found lateral to the VA cells in the caudal mc. The +Y and −X−Z cells are found lateral to the rostralmost VA cells and the H-135 cells. The distribution of H-135 cells does not extend to the most rostral margin of the mc. That is, most of the −Y cells are not bordered medially by H-135 cells. The projection of this rostral-medial margin of the mc remains unknown.

Comparative considerations

Wylie et al. (1999) noted a striking similarity in the organization of the rotational optic flow system in pigeons and mammals. In the IO of mammals, the input to the VA zones in the VbC is from the caudal dorsal cap, whereas the input to the H-135 zones is from the rostral dorsal cap and ventrolateral outgrowth (Ruigrok et al., 1992; Tan et al., 1995). Similarly, in pigeons, the input to the VA and H-135 zones is from the caudal and rostral margins of the medial mc, respectively. The results of the present study are not comparable with mammals. Cells responsive to translational optic flow have not been identified in the VbC of mammals (but see Shojaku et al., 1991; Barmack and Shojaku, 1992, 1995).

The accessory optic/pretectal-olivo-cerebellar pathway

In birds, the optic flow input to the mc arises from two retinal recipient structures: the nucleus of the basal optic root (nBOR) of the accessory optic system, and the pretectal nucleus lentiformis mesencephali (LM; Clarke, 1977; Karten et al., 1977; Brecha et al., 1980; Gamlin and Cohen, 1988a,b; Wylie et al., 1997). Most neurons in the nBOR and LM have monocular receptive fields and exhibit direction selectivity in response to largefield stimuli (Burns and Wallman, 1981; Morgan and Frost, 1981; Winterson and Brauth, 1985; Wylie and Frost, 1990). Most neurons in nBOR prefer either upward (U), downward (D), or backward (nasal to temporal; B) motion in the contralateral visual field (Wylie and Frost, 1990), whereas most LM neurons prefer forward (F) motion in the contralateral visual field (Winterson and Brauth, 1985). The LM projects to the ipsilateral mc (Clarke, 1977; Gamlin and Cohen, 1988b). The nBOR projects bilaterally to the mc, but the projection is heavier to the ipsilateral side (Brecha et al., 1980; Wylie et al., 1997). At the mc, the neurons have binocular receptive fields and respond best to particular patterns of optic flow resulting from self-translation and self-rotation, as we have described above. (This is inferred from the fact that the complex spike activity of Purkinje cells, which reflects CF input from the contralateral IO, responds to these patterns of optic flow; Wylie and Frost, 1993, 1999.)

Based on the results of the present study and Wylie et al. (1999), we predict that the input to the caudal mc would be mainly from the LM, and the input to the rostral mc would be mainly from the nBOR. In Figure 7, we show the receptive field structure of IO neurons, topographically organized, and a schematic of the transmission of information from the retina to the nBOR and LM, and then to mc. For the different types of cells in the mc, we show the direction of largefield motion in different regions of the optimal flowfield. The caudal mc contains VA and −X−Z cells. VA cells in the right mc prefer B motion in the ipsilateral hemifield, and F motion in the contralateral
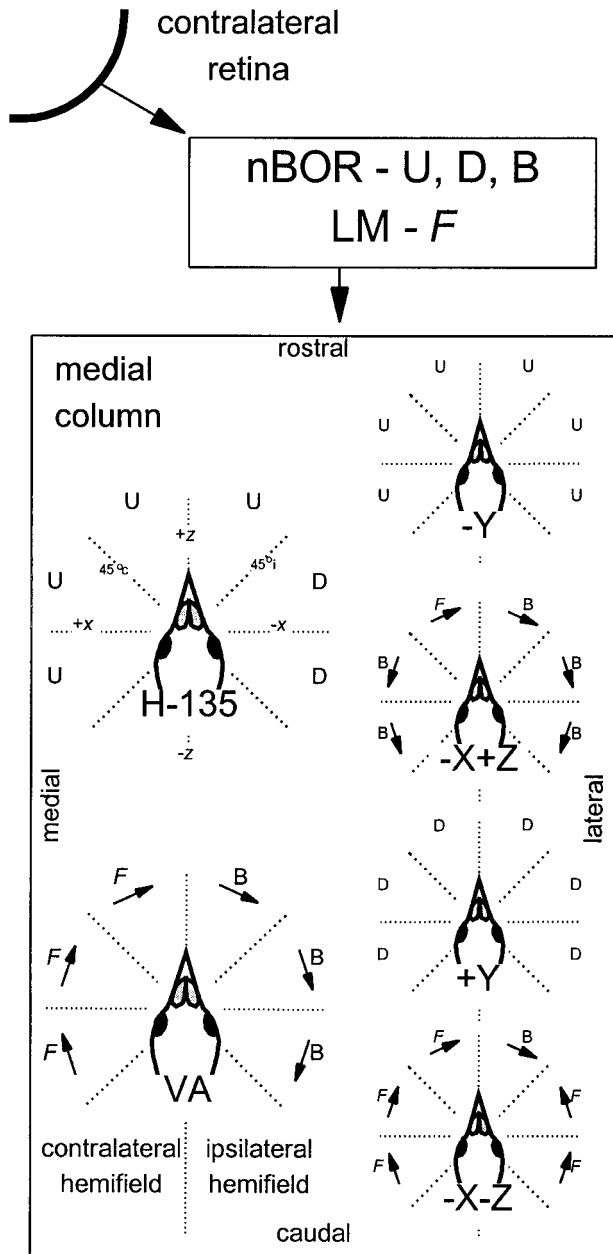
Fig. 7. A schematic of the organization of the medial column (mc) in pigeons. This figure shows the receptive field structure of the cell types in the mc on the right side of the brain, topographically organized. For each cell type, the optimal flowfield is simplified: the direction of motion that occurs in different parts of the binocular visual field (along the "equator" of the flowfield) is shown. The transmission of information from the contralateral retina, through the nucleus of the basal optic root (nBOR) and nucleus lentiformis mesencephali (LM), is also indicated. U, D, F, B = upward, downward, forward (temporal to nasal) and backward motion, respectively. See text for a detailed discussion. VA, vertical axis.

most LM neurons prefer F motion in the contralateral eye (Winterson and Brauth, 1985). As such, one would predict that the caudal mc is heavily innervated by the ipsilateral LM. The other cell types have direction preferences that suggest the rostral mc is more heavily innervated by the nBOR. Respectively, −Y and +Y cells prefer U and D motion throughout both hemifields. H-135 cells prefer U motion throughout the contralateral hemifield and anterior quadrant of the ipsilateral hemifield, and downward motion in the central and posterior regions of the ipsilateral hemifield. −X−Z cells prefer B motion throughout the ipsilateral hemifield and the central and posterior regions of the contralateral hemifield, and F motion in the anterior quadrant of the contralateral hemifield. Given that the nBOR has neurons that prefer either U, D, or B motion in the contralateral eye, one would expect a predominant input from the nBOR to the rostral mc. In summary, the topographic organization of the pigeon mc suggests that the nBOR and LM would project primarily to the rostral and caudal regions of the mc, respectively. Indeed, a similar pattern of connectivity has been found in mammals. The avian nBOR is homologous to the medial and lateral terminal nuclei (MTN/LTN) in mammals, and the LM is homologous to the nucleus of the optic tract (NOT; Simpson, 1984; Simpson et al., 1988). The projection from the NOT to the IO is predominantly to the caudal dorsal cap, and the projection to the rostral dorsal cap is from the visual tegmental relay zone, which receives input from the MTN/LTN (Takeda and Maekawa, 1976; Maekawa and Takeda, 1979; Giolli et al., 1985).

ACKNOWLEDGMENTS

LITERATURE CITED

Arends JJA, Voogd J. 1989. Topographic aspects of the olivocerebellar system in the pigeon. Exp Brain Res Suppl 17:52–57.

Arends JJA, Zeigler HP. 1991. Organization of the cerebellum in the pigeon (*Columba livia*). I. Corticonuclear and corticovestibular connections. J Comp Neurol 306:221–244.

Barmack NH, Shojaku H. 1992. Representation of a postural coordinate system in the nodulus of the rabbit cerebellum by vestibular climbing fiber signals. In: Shimazu H, Shimoda Y, editors. Vestibular control of eye, head and body movements. Basel: Japan Scientific Societies Press, Tokyo/ S. Karger. p 331–338.

Barmack NH, Shojaku H. 1995. Vestibular and visual climbing fiber signals evoked in the uvula-nodulus of the rabbit cerebellum by natural stimulation. J Neurophysiol 74: 2573–2589.

Brecha NC, Karten HJ, Hunt SP. 1980. Projections to the nucleus of the basal optic root in the pigeon: an autoradiographic and horseradish peroxidase study. J Comp Neurol 189:615–670.

Burns S, Wallman J. 1981. Relation of single unit properties to the occulomotor function of the nucleus of the basal optic root (AOS) in chickens. Exp Brain Res 42:171–180.

Clarke PGH. 1977. Some visual an other connections to the cerebellum of the pigeon. J Comp Neurol 174:535–552.

Gamlin PDR, Cohen DH. 1988a. The retinal projections to the pretectum in the pigeon (*Columba livia*). J Comp Neurol 269:1–17.

Gamlin PDR, Cohen DH. 1988b. Projections of the retinorecipient pretectal nuclei in the pigeon (*Columba livia*). J Comp Neurol 269:18–46.

Gibson JJ. 1954. The visual perception of object motion and subjective movement. Psychol Rev 61:304–314.

hemifield. −X−Z cells prefer F motion throughout contralateral hemifield, F motion in the central and posterior regions of the ipsilateral hemifield, and B motion in the anterior quadrant of the ipsilateral hemifield. Recall that

Giolli RA, Blanks RHI, Torigoe Y, Williams DD. 1985. Projections of the medial terminal accessory optic nucleus, ventral tegmental nuclei, and substantia nigra of rabbit and rat as studied by retrograde axonal transport of horseradish peroxidase. J Comp Neurol 232:99–116.

Graf W, Simpson JI, Leonard CS. 1988. Spatial organization of visual messages of the rabbit's cerebellar flocculus. II. Complex and simple spike responses of Purkinje cells. J Neurophysiol 60:2091–2121.

Karten HJ, Hodos W. 1967. A stereotaxic atlas of the brain of the pigeon (*Columba livia*). Baltimore: Johns Hopkins University Press.

Karten HJ, Fite KV, Brecha N. 1977. Specific projection of displaced retinal ganglion cells upon the accessory optic system in the pigeon (*Columba livia*). Proc Natl Acad Sci USA 74:1752–1756.

Larsell O. 1948. The development and subdivisions of the cerebellum of birds. J Comp Neurol 89:123–190.

Larsell O, Whitlock DG. 1952. Further observations on the vestibulocerebellum of birds. J Comp Neurol 97:545–566.

Lau KL, Glover RG, Linkenhoker B, Wylie DRW. 1998. Topographical organization of the inferior olive cells projecting to translation and rotation zones in the vestibulocerebellum of pigeons. Neuroscience 85:605–614.

Maekawa K, Takeda T. 1979. Origin of descending afferents to the rostral part of the dorsal cap inferior olive which transfers contralateral optic activities to the flocculus. A horseradish preoxidase study. Brain Res 172:393–405.

Morgan B, Frost BJ. 1981. Visual response properties of neurons in the nucleus of the basal optic root of pigeons. Exp Brain Res 42:184–188.

Ruigrok TJH, Osse RJ, Voogd J. 1992. Organization of the inferior olivary projections to the flocculus and ventral paraflocculus of the rat cerebellum. J Comp Neurol 316:129–150.

Shojaku H, Barmack NH, Mizukoshi K. 1991. Influence of vestibular and visual climbing fiber signals on Purkinje cell discharge in the cerebellar nodulus of the rabbit. Acta Otolaryngol Suppl 481:242–246.

Simpson JI. 1984. The accessory optic system. Rev Neurosci 7:13–41.

Simpson JI, Graf W, Leonard CI. 1981. The coordinate system of visual climbing fibers to the flocculus. In: Fuchs AF, Becker W, editors. Progress in occulomotor research. Amsterdam: Elsevier. p 475–485.

Simpson JI, Leonard CS, Soodak RE. 1988. The accessory optic system: II. spatial organization of direction selectivity. J Neurophysiol 60:2055–2072.

Takeda T, Maekawa K. 1976. The origin of the pretecto-olivary tract. A study using the horseradish peroxidase method. Brain Res 117:319–325.

Tan J, Epema AH, Voogd J. 1995. Zonal organization of the flocculovestibular nucleus projection in the rabbit. A combined axonal tracing and acetylcholinesterase histochemical study. J Comp Neurol 356:51–71.

Vogt-Nilson L. 1954. The inferior olive in birds. A comparative morphological study. J Comp Neurol 101:447–481.

Whitlock DG. 1952. A neurohistological and neuropsychological study of afferent fiber tracts and receptive areas of the avian cerebellum. J Comp Neurol 97:567–635.

Wild JM. 1993. Descending projections of the songbird nucleus robustus archistrialis. J Comp Neurol 338:225–241.

Winterson BJ, Brauth SE. 1985. Direction selective single units in the nucleus lentifomis mesencephali of the pigeon (*Columba livia*). Exp Brain Res 60:215–226.

Wylie DRW, Frost BJ. 1990. Visual response properties of neurons in the nucleus of the basal optic root of the pigeon: a quantitative analysis. Exp Brain Res 82:327–336.

Wylie DRW, Frost BJ. 1993. Responses of vestibulocerebellar neurons to optokinetic stimulation: II. the 3-dimensional reference frame of rotation neurons in the flocculus. J Neurophysiol 70:2632–2646.

Wylie DRW, Frost BJ. 1999. Complex spike activity of purkinje cells in the ventral uvula and nodulus of pigeons in response to translational optic flow. J Neurophysiol 81:256–266.

Wylie DRW, Kripalani T, Frost BJ. 1993. Responses of vestibulocerebellar neurons to optokinetic stimulation: I. functional organization of neurons discriminating between translational and rotational visual flow J Neurophysiol 70:2632–2646.

Wylie DRW, Linkenhoker B, Lau KL. 1997. Projections of the nucleus of the basal optic root in pigeons (*Columba livia*) revealed with biotinylated dextran amine. J Comp Neurol 384:517–536.

Wylie DRW, Bischof WF, Frost BJ. 1998. Common reference frame for neural coding of translational and rotational optic flow. Nature 392:278–282.

Wylie DRW, Winship IR, Glover RG. 1999. Projections from the medial column of the inferior olive to different classes of rotation-sensitive Purkinje cells in the flocculus of pigeons. Neurosci Lett 268:97–100.